Cone-shaped forest of aligned carbon nanotubes: An alternative probe for scanning microscopy

Zhiming Xiao, Mirza Saquib Sarwar, Masoud Dahmardeh, Mehran Vahdani Moghaddam, Alireza Nojeh, and Kenichi Takahata

Citation: Applied Physics Letters **103**, 171603 (2013); doi: 10.1063/1.4826518
View online: http://dx.doi.org/10.1063/1.4826518
View Table of Contents: http://scitation.aip.org/content/aip/journal/apl/103/17?ver=pdfcov
Published by the AIP Publishing

Cone-shaped forest of aligned carbon nanotubes: An alternative probe for scanning microscopy

Zhiming Xiao, Mirza Saquib Sarwar, Masoud Dahmardeh, Mehran Vahdani Moghaddam, Alireza Nojeh,[a] and Kenichi Takahata[b]
Department of Electrical and Computer Engineering, University of British Columbia, Vancouver, British Columbia V6T 1Z4, Canada

(Received 6 September 2013; accepted 8 October 2013; published online 22 October 2013)

A scanning microscopy probe based on three-dimensionally shaped carbon nanotube (CNT) forests and its application to atomic-force microscopy (AFM) are reported. Micro-scale CNT forests directly grown on silicon cantilevers are patterned into cone shapes with the tips of a few individual nanotubes. The CNT-forest-based probes provide significantly higher mechanical stability/robustness than the common single-CNT probes. AFM imaging using the fabricated probes reveals their imaging ability comparable to that of commercial probes. The patterning process also improves the uniformity of the CNT forests grown on each cantilever. The results suggest a promising future for CNT scanning probes and their production approach. © *2013 AIP Publishing LLC*. [http://dx.doi.org/10.1063/1.4826518]

Atomic force microscopy (AFM) nowadays plays a core role in materials science, surface physics, and biology, to name a few disciplines. The technique is considered as one of the most important inventions in materials science.[1] Generally speaking, AFM is one form of the scanning probe microscope, which, as the name explains, uses a scanning probe to map the surface topography of samples.[2] The probe typically has a micro-scale cantilever with a sharp tip formed at its end. The cantilever serves as a transducer that is used to detect the force signal exerted by the interaction between the probe tip and the sample surface. Typical materials used for AFM probes are silicon (Si) and silicon nitride (Si_3N_4). These cantilever probes with desired spring constants and resonant frequency, morphology, and sharp tips can be mass-produced using micro-electro-mechanical systems (MEMS) technology. However, manufacturing AFM probes with high reproducibility in dimensional control of 10 nm or below at reasonable costs still remains a major challenge.[3] In the full/intermittent contact mode, the geometry of the tip changes during the scanning process due to mechanical wear of the tip, deteriorating the quality of AFM images. Therefore, alternative materials are required for AFM probes with improved performance. Carbon nanotubes (CNTs) have well-defined nano-scale geometry and, with three times the stiffness of Si, exhibit much higher wear resistance than that of Si.[4] CNTs are therefore considered as one of the most promising candidates for AFM probe materials. CNT probes are commercially available and are currently produced through two main methods: assembly of a CNT at the tip of a micro-machined Si structure and direct growth of a CNT on a Si tip using chemical vapor deposition (CVD). The former is not only time-consuming but also needs expensive auxiliary instruments, such as a scanning electron microscope (SEM), to perform the nano-scale assembly in a precise and systematic manner.[5–7] The latter method eliminates the need for assembly, which is promising in achieving relatively fast and low-cost fabrication of the probes.[8–10] However, the control of CNT growth, including the orientation, the number of CNTs formed on each cantilever, and the wafer-scale uniformity of grown CNTs, still remains an essential issue. In this report, an alternative, potentially low-cost, and wafer-scale method for manufacturing of CNT-based AFM probes is presented. Micro-scale arrays or "forests" of vertically aligned CNTs are grown directly on tipless Si cantilevers. The CNT forests are then three-dimensionally (3D) patterned into cone shapes to be used as AFM probe tips. Dry micro-electro-discharge machining (μEDM) is employed for this 3D patterning.[11–13] The results from AFM imaging tests performed using the fabricated CNT probes show a promising potential of this AFM probe and its production approach.

To create the CNT-forest probe and ensure its compatibility with AFM systems, we utilized a commercially available tipless Si cantilever probe (ACL-TL, Applied NanoStructures, Inc., CA, USA) and grew the CNT forest at the free end of the cantilever using an atmospheric-pressure CVD system.[11,14] For this, first, the tipless probe was covered by a shadow mask except for the end of the cantilever where the catalyst layer (1-nm-thick iron on 10-nm-thick alumina) was deposited using electron-beam evaporation (Fig. 1(a)). The length of the exposed cantilever was adjusted to be 50 μm to 150 μm. After the catalyst formation, the AFM probe was transferred to the reaction tube of the CVD system to synthesize a CNT forest with a height of $\sim$100 μm using ethylene as the carbon source (Fig. 1(b)). Details of the CVD process are given elsewhere.[11,14] Dry μEDM was performed in the CNT forest to fabricate a cone-shaped probe using a servo-controlled 3-axis μEDM system with 100-nm positioning resolution (EM203, SmalTec International, IL, USA); the experimental setup used for this process is illustrated in Fig. 1(c). μEDM is a micromachining process that utilizes pulses of thermomechanical impact induced by an extremely miniaturized electrical discharge generated between a micro-scale electrode and a workpiece, which is a CNT forest in this

[a]Electronic mail: anojeh@ece.ubc.ca
[b]Electronic mail: takahata@ece.ubc.ca

study. As shown Fig. 1(c), the system uses a relaxation-type resistor-capacitor circuit as a proven discharge pulse generator.[15] In typical μEDM, the workpiece is submerged in dielectric liquid (commonly oil or ultrapure water) to perform the removal process; this process ambient assists flushing of debris produced during the process. The CNT forest as the workpiece of μEDM, however, cannot be immersed in liquid because the aligned CNTs collapse when the wetted forest is dried due to the capillary force effect.[11] Therefore, CNT forests are μEDMed in dry ambient, with oxygen mixed with inert gas, which enables precise etching of the nanotubes using microscopic tool electrodes by establishing the pulses of micro discharge between the electrode and the forest.[11–13] A detailed study suggested that dry μEDM of CNT forest was essentially oxygen plasma etching rather than the conventional, direct thermal removal (evaporation and melting) process and that air (or nitrogen with ~20% oxygen) was an optimal medium for the process.[13] With numerical control of the electrode position with respect to the forest, 3D, free-form patterning of the material is enabled. In addition, parallel μEDM that uses arrays of electrode can potentially be applied to batch production of CNT AFM probes for industrial manufacturing of the products.[16]

The patterning of a cone shape in the grown CNT forest was performed as follows. The AFM probe with a CNT forest grown at the end of the cantilever was fixed on a piece of metal sheet, which was then mounted on the stage of the μEDM system to electrically couple the probe with the discharge circuitry of the system. In the past studies, the electrical connection to a CNT forest was made by clamping the sample directly on the forest surface in order to minimize the electrical resistance in the circuitry.[11–13] This method was not available for the current case as the cantilever on which the CNT forest was present was highly flexible and fragile. Therefore, the electrical connection to the forest was made through the bottom of the cantilever probe in a manner described above. In order to minimize the resistance, the Si of the cantilever was selected to be a highly doped type. To create a cone shape in the forest material, a tungsten electrode with a diameter of 300 μm was shaped into a 200-μm-long, circularly truncated cone (Fig. 2(a)) using a wire electro-discharge grinding (WEDG) technique.[17] The precise alignment of the tungsten electrode and the CNT forest was achieved using the microscope available with the system. The patterning process was then initiated in air using a discharge voltage of 50 V. This discharge voltage, which is higher than the voltage level previously reported (30 V),[11] was observed to be optimal in terms of the quality of machined forest surfaces in the present case; a potential reason behind this outcome is that the higher voltage was necessary to overcome the relatively higher resistance (caused by the electrical connection to the forest through the Si structure as noted above) compared with the previous case (with the direct contact to the forest) and maintain sufficient discharge currents for smooth CNT removal. The sample was continuously moved along a circular orbit with a fixed radius of 45 μm using the X-Y stage of the system while feeding the electrode with the Z stage until it reached a target depth. In this process, the CNTs along the electrode path were removed, forming a cone shape in the forest. Initially during the process, a truncated cone was formed as shown in Fig. 2(c). As removal proceeded, the radius of the topside of the truncated cone kept decreasing until it reached a sharp tip (Fig. 2(d)). As the slope angle of the electrode's sidewalls is constant, the height of the cone obtained depends on the radius of the circular orbit. The combination of the particular electrode's slope and orbit radius leads to the cone's height of 70 μm. Fig. 3(a) displays a result of μEDM patterning, showing a cone created in the CNT forest on the Si cantilever (this structure is named probe 1 in later discussions). The apex radius of the cone was measured to be approximately 2.5 μm. The target and measured geometrical parameters of the created cone are summarized in Table I. Compared with commercial CNT AFM probes, in which a single CNT is commonly used as the probe tip fixed on a cantilever, the cone-shaped CNT-forest probes have higher mechanical stability/robustness due to their unique structure. The CNTs, whose tips make direct contact with the samples to be probed, are in the central region of the cone. The outer CNTs that surround the central CNTs have densities (estimated to be $\sim 10^{15}/m^2$ with an average distance of a few tens of nanometers between neighboring CNTs[18]) high enough to physically support and protect the central ones. Furthermore, those CNTs are entangled with each other, leading to constraining forces among the CNTs that tie them as a whole and further enhance the physical supporting effect. Although the contact between an individual CNT and the substrate may be weak, the contact of the CNT forest as a whole with the substrate (cantilever in this case) is strong. Therefore, the mechanical stability and robustness of these CNT probes are expected to be much higher than those available with conventional CNT probes fabricated with other methods described earlier, potentially enabling significantly improved reliability and longevity in CNT-based AFM probes.

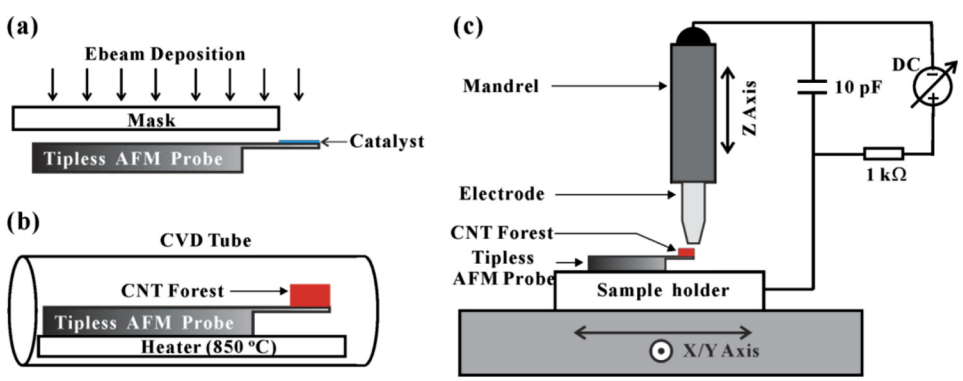

FIG. 1. Illustration of fabrication processes and set-ups used: (a) catalyst deposition on the cantilever, (b) CNT forest growth in the CVD tube, and (c) μEDM setup.

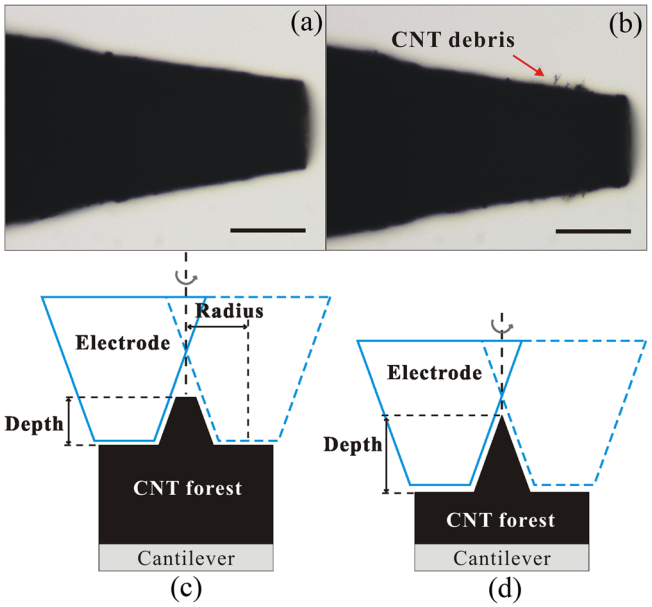

FIG. 2. (a) Tapered tungsten electrode used for μEDM and (b) the electrode immediately after the process (but before the cleaning step) showing CNT debris adhered on the electrode surface. Scale bars are 50 μm. Illustration of the cone-shaping process at (c) a transient state with a truncated cone shape formed in the CNT forest and (d) the final stage of the process in which the forest is shaped to a sharp-tip cone.

Theoretically, the developed process can produce a cone tip containing a single CNT only. However, as the CNT forest is machined in the dry μEDM process, some of the debris of the removed CNTs tends to adhere to the electrode (as shown in Fig. 2(b)) potentially due to less flushing effects compared with traditional wet μEDM that is performed in liquid.[11] As the carbon debris is electrically conductive, those stuck on the electrode essentially can serve as parts of the electrode and contribute to the removal of the forest in an unpredictable manner. This removal effect can also occur at the apex of the cone, deteriorating the sharpness of the cone's tip. This condition was present in the case of the probe 1 device (Fig. 3(a)). In order to avoid this type of impact caused by the debris and maximize the integrity of the cone structure, we developed and utilized a multi-step fabrication process. In this process, a larger cone pattern was first shaped by the process discussed earlier. The electrode was then cleaned to remove any debris stuck on it. Next, this electrode was used to remove the surface layer of the cone using a smaller-radius circular orbit, followed by electrode cleaning again. This set of surface layer removal and electrode cleaning was repeated until the cone was carved to have a very sharp apex. The removal thickness in each step in this process was 3-5 μm, and this thickness was reduced to 0.5-1 μm at the final steps for finishing purposes. The gap clearance between the electrode and a CNT forest during the fabrication process was measured to be approximately 5 μm, and the scanning paths of the electrode were compensated with this gap to obtain the final structure with desired geometry. A bottom layer of the forest (with a thickness of less than 30 μm) was left unpatterned in order to eliminate any possibility of damaging the Si cantilever during the forest shaping. Figs. 3(b) and 3(c) show the results obtained through the multi-step process described above. It can be

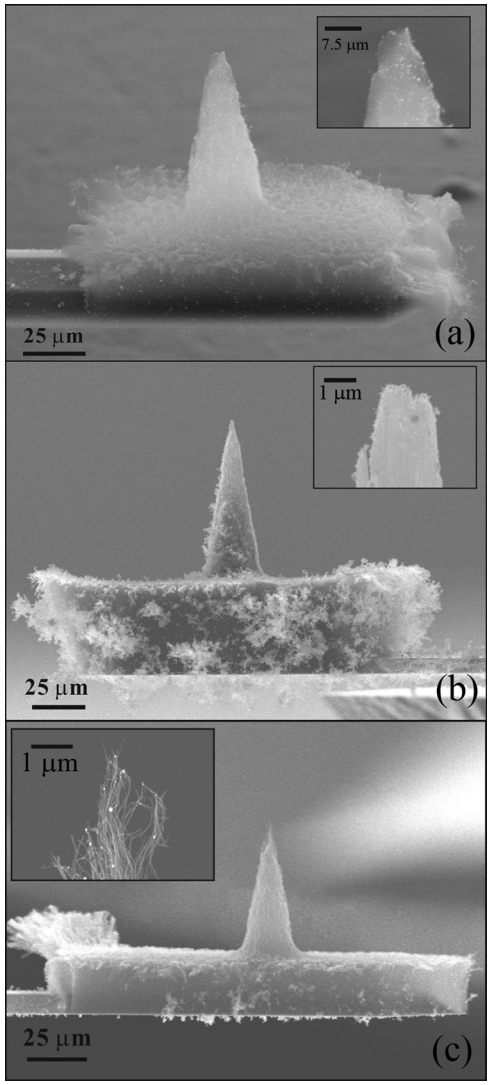

FIG. 3. SEM images of the CNT probes fabricated: (a) probe 1, (b) probe 2, and (c) probe 3.

seen that the radius of the tip in Fig. 3(b) (probe 2) is less than 1 μm and that the tip in Fig. 3(c) (probe 3) has only two CNTs at the apex, verifying that the modified process is effective in producing finer tips in the cone structures compared with the single-step process discussed earlier. The designed and measured geometries of these two probes are also shown in Table I, indicating that all the cases show good matches but with higher tolerances (of $\sim$3 μm in radius and $\sim$5 μm in height) in the structures machined with the multi-step process (probes 2 and 3), consistent with the observations in the SEM images. The difference in the tip shapes between these two cases might be related to some small level of the debris still remaining on the electrode and/or fluctuation in pulse energy; these factors ultimately define the patterning resolution. It should also be noted that the difference in the thickness of the unpatterned bottom layers of the CNT forests among the probes is due to the difference in the heights of as-grown forests as well as that in the depths of removal performed in the forests.

Precise control of the height of CNT forests in CVD growth still remains an unsolved essential issue. Even if we initiate the synthesis of CNTs on multiple probes at the same

TABLE I. Designed and measured geometrical parameters of the CNT probe.

	Probe 1	Probe 2	Probe 3
Orbit radius (μm)	45	43	40
Designed bottom radius and height (μm)	20/70	18/70	15/60
Measured bottom radius and height (μm)	15/80	15/74.9	11/54.5
Measured apex radius (μm)	~2.5	<1	~0.02 (diameter of CNTs)

time in the same reaction tube, the heights of the forests grown on the probes could be different from each other. Thus, achieving high uniformity of individual CNTs on the cantilever in terms of their final height is a great challenge if direct CVD growth is used to define the CNT probes. Post-growth treatments can be introduced to improve the uniformity.[7] However, these treatments not only are time-consuming but also need rather expensive systems to perform, posing practical issues in product manufacturing. Here, the developed μEDM process for cone patterning is directly applicable for customizing the final height of the CNT probes, to be precisely determined as part of the cone shaping process, addressing the non-uniformity issue. This can be easily achieved by, e.g., setting the end of electrode feeding in the Z direction with respect to the top surface of the cantilever, instead of that of the forest whose height can vary, eliminating the impact of the forest's height variation on the heights of the final structures (both cone and bottom layer) patterned on the cantilever.

AFM imaging was performed using probes 2 and 3 (Figs. 3(b) and 3(c), respectively) in a commercially available AFM system (Easyscan 2, Nanosurf, Liestal, Switzerland). In order to evaluate the imaging ability of the fabricated CNT probes, we conducted the same imaging using a commercial Si probe (ACL-A, Applied NanoStructures, Inc., CA, USA; typical tip radius ~6 nm, apex half cone angle 11°, resonant frequency ~184 kHz). The tapping mode was used in these AFM tests, in which each probe was scanned over a standard calibration sample that has an array of 5-μm square dimples with a depth of 98 nm. In the developed probes, the presence

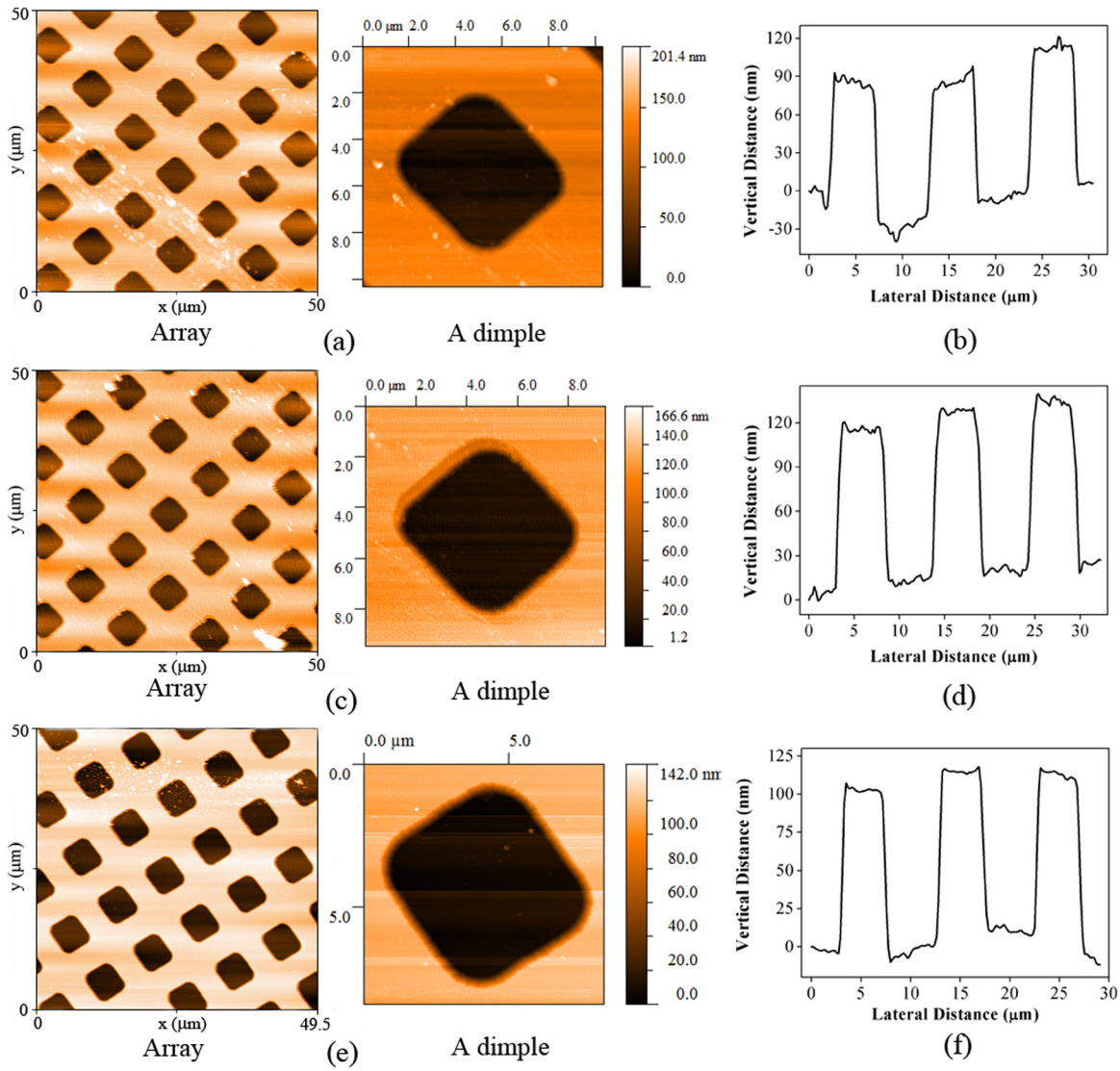

FIG. 4. AFM images of calibration microstructures measured using (a) probe 2, (c) probe 3, and (e) commercial Si probe. Corresponding cross-sectional profiles of multiple dimples are shown in (b), (d), and (f), respectively.

TABLE II. R_{RMS} values of calibration dimple structures measured using fabricated CNT probes and commercial probe.

R_{RMS} (nm)		Probe 2	Probe 3	Commercial probe
Area	Bottom	5.9	2.7	4.3
	Top	4.6	3.4	2.5
Line	Bottom	2.7	2.5	2.0
	Top	3.1	2.5	1.6

of the CNTs on the cantilever decreased the resonant frequency of the cantilever. The rated nominal resonant frequency of the tipless probe used is 190 kHz, and this frequency was measured to be modified to 136 kHz and 170 kHz for probes 2 and 3, respectively. The difference between these resonant frequencies of probes 2 and 3 is presumed to be mainly associated with the difference in the thickness of the bottom layers of the forests (i.e., probe 2 has a thicker bottom layer and thus a higher mass, leading to the lower resonant frequency compared with probe 3). The AFM results are presented in Figs. 4(a)–4(f). The AFM images of an identical region of the calibration sample obtained using probes 2 and 3 are shown in Figs. 4(a) and 4(c), respectively, and those with the commercial probe are shown in Fig. 4(e). Corresponding cross-sectional profiles of the identical dimples obtained in the imaging process are also shown in Figs. 4(b), 4(d), and 4(f). Comparing between the results with the developed CNT probes and that with the commercial one, it is clear that the CNT probes were able to trace the contour of this square patterns similarly to the commercial probe. The root mean squared area/line roughness of the bottom surface of a single dimple and the top surface of the sample (between two dimples) was characterized. As shown in Table II, the results obtained with probe 2 are somewhat larger than those with the commercial probe. We can see that the roughness obtained by probe 3 is close to that of the commercial probe. The difference in these outcomes could be associated with that in the radius of the two probes. Nevertheless, the results demonstrate that the fabricated CNT probes can produce scanned data comparable to those that the commercial probe does in AFM imaging of micro-scale patterns with nano-scale steps. The machining process is being improved to achieve finer probe tips and higher lateral resolutions in AFM imaging.

In summary, we have demonstrated that dry μEDM is highly effective in producing CNT-forest AFM probes with custom cone-shaped designs. The probe shaping process was performed on the CNT forests that were grown directly on the tips of Si cantilevers compatible with commercial AFM systems. This approach potentially enables CNT-based AFM probes to have remarkably higher mechanical stability and robustness, as well as to be batch manufactured with higher dimensional precisions at low costs through a path of parallel μEDM. The results of AFM imaging obtained with the fabricated probes encourage further improvement of the probe and AFM imaging with it through nano-meter level dimension control and finishing of the probe tips.

This work was partially supported by the Natural Sciences and Engineering Research Council of Canada, the Canada Foundation for Innovation, the British Columbia Knowledge Development Fund, and the BCFRST Foundation/British Columbia Innovation Council. K. Takahata was supported by the Canada Research Chairs program.

[1]J. Wood, Mater. Today **11**, 40 (2008).
[2]P. Eaton and P. West, *Atomic Force Microscopy* (Oxford University Press, New York, 2010), pp. 1–6.
[3]N. Wilson and J. Macpherson, Nat. Nanotechnol. **4**, 483 (2009).
[4]B. C. Park, J. Choi, S. J. Ahn, D.-H. Kim, J. Lyou, R. Dixson, N. G. Orji, J. Fu, and T. V. Vorburger, Proc. SPIE **6518**, 651819 (2007).
[5]H. Dai, J. H. Hafner, A. G. Rinzler, D. T. Colbert, and R. E. Smalley, Nature **384**, 147 (1996).
[6]N. deJonge, Y. Lamy, and M. Kaiser, Nano Lett. **3**, 1621 (2003).
[7]J. Martinez, T. D. Yuzvinsky, A. M. Fennimore, A. Zettl, R. García, and C. Bustamante, Nanotechnology **16**, 2493 (2005).
[8]J. H. Hafner, C. L. Cheung, and C. M. Lieber, Nature **398**, 761 (1999).
[9]J. H. Hafner, C. L. Cheung, and C. M. Lieber, J. Am. Chem. Soc. **121**, 9750 (1999).
[10]E. Yenilmez, Q. Wang, R. J. Chen, D. Wang, and H. Dai, Appl. Phys. Lett. **80**, 2225 (2002).
[11]W. Khalid, M. S. M. Ali, M. Dahmardeh, Y. Choi, P. Yaghoobi, A. Nojeh, and K. Takahata, Diamond Relat. Mater. **19**, 1405 (2010).
[12]T. Saleh, M. Dahmardeh, A. Bsoul, A. Nojeh, and K. Takahata, J. Appl. Phys. **110**, 103305 (2011).
[13]M. Dahmardeh, A. Nojeh, and K. Takahata, J. Appl. Phys. **109**, 093308 (2011).
[14]M. V. Moghaddam, P. Yaghoobi, and A. Nojeh, Appl. Phys. Lett. **101**, 253110 (2012).
[15]M. P. Jahan, Y. S. Wong, and M. Rahman, J. Mater. Process. Technol. **209**, 1706 (2009).
[16]K. Takahata and Y. B. Gianchandani, J. Microelectromech. Syst. **11**, 102 (2002).
[17]T. Masuzawa, M. Fujino, K. Kobayashi, T. Suzuki, and N. Kinoshita, CIRP Ann. **34**, 431 (1985).
[18]Md. K. Alam, P. Yaghoobi, and A. Nojeh, Scanning **31**, 221 (2009).